NASA/TM—2002-211297 AIAA–2001–3233

Solid Hydrogen Experiments for Atomic Propellants: Image Analyses

Bryan Palaszewski
Glenn Research Center, Cleveland, Ohio

January 2002

The NASA STI Program Office . . . in Profile

Since its founding, NASA has been dedicated to the advancement of aeronautics and space science. The NASA Scientific and Technical Information (STI) Program Office plays a key part in helping NASA maintain this important role.

The NASA STI Program Office is operated by Langley Research Center, the Lead Center for NASA's scientific and technical information. The NASA STI Program Office provides access to the NASA STI Database, the largest collection of aeronautical and space science STI in the world. The Program Office is also NASA's institutional mechanism for disseminating the results of its research and development activities. These results are published by NASA in the NASA STI Report Series, which includes the following report types:

- TECHNICAL PUBLICATION. Reports of completed research or a major significant phase of research that present the results of NASA programs and include extensive data or theoretical analysis. Includes compilations of significant scientific and technical data and information deemed to be of continuing reference value. NASA's counterpart of peer-reviewed formal professional papers but has less stringent limitations on manuscript length and extent of graphic presentations.

- TECHNICAL MEMORANDUM. Scientific and technical findings that are preliminary or of specialized interest, e.g., quick release reports, working papers, and bibliographies that contain minimal annotation. Does not contain extensive analysis.

- CONTRACTOR REPORT. Scientific and technical findings by NASA-sponsored contractors and grantees.

- CONFERENCE PUBLICATION. Collected papers from scientific and technical conferences, symposia, seminars, or other meetings sponsored or cosponsored by NASA.

- SPECIAL PUBLICATION. Scientific, technical, or historical information from NASA programs, projects, and missions, often concerned with subjects having substantial public interest.

- TECHNICAL TRANSLATION. English-language translations of foreign scientific and technical material pertinent to NASA's mission.

Specialized services that complement the STI Program Office's diverse offerings include creating custom thesauri, building customized data bases, organizing and publishing research results . . . even providing videos.

For more information about the NASA STI Program Office, see the following:

- Access the NASA STI Program Home Page at ***http://www.sti.nasa.gov***

- E-mail your question via the Internet to help@sti.nasa.gov

- Fax your question to the NASA Access Help Desk at 301–621–0134

- Telephone the NASA Access Help Desk at 301–621–0390

- Write to:
  NASA Access Help Desk
  NASA Center for AeroSpace Information
  7121 Standard Drive
  Hanover, MD 21076

NASA/TM—2002-211297

AIAA–2001–3233

Solid Hydrogen Experiments for Atomic Propellants: Image Analyses

Bryan Palaszewski
Glenn Research Center, Cleveland, Ohio

Prepared for the
37th Joint Propulsion Conference and Exhibit
cosponsored by the AIAA, ASME, SAE, and ASEE
Salt Lake City, Utah, July 8–11, 2001

National Aeronautics and
Space Administration

Glenn Research Center

January 2002

Acknowledgments

I would like to thank the people who assisted in the construction and execution of the experiments conducted at NASA Glenn Research Center: Maureen Kudlac (GRC), Henry Speier, Joan Hoopes, Ernie Bell, Donald Metcalf, and Robert Vanek. Thanks to Hugh Aylward for the image capturing and pixel measurements of the particle sizes. I would also like to thank John Cole, head of Space Transportation Research (STR) aspects of the NASA Advanced Space Transportation Program (ASTP), led by NASA Marshall Space Flight Center. Extensive cooperation with the USAF Research Laboratory (Edwards, CA) was also a critical part of this testing.

Available from

NASA Center for Aerospace Information
7121 Standard Drive
Hanover, MD 21076

National Technical Information Service
5285 Port Royal Road
Springfield, VA 22100

Available electronically at http://gltrs.grc.nasa.gov/GLTRS

SOLID HYDROGEN EXPERIMENTS FOR ATOMIC PROPELLANTS: IMAGE ANALYSES

Bryan Palaszewski
National Aeronautics and Space Administration
Glenn Research Center
Cleveland, Ohio 44135
216–977–7493 Voice
216–433–5802 FAX
bryan.a.palaszewski@grc.nasa.gov
Fuels and Space Propellants Web Site
http://www.grc.nasa.gov/WWW/TU/launch/foctopsb.htm

ABSTRACT

This paper presents the results of detailed analyses of the images from experiments that were conducted on the formation of solid hydrogen particles in liquid helium. Solid particles of hydrogen were frozen in liquid helium, and observed with a video camera. The solid hydrogen particle sizes, their agglomerates, and the total mass of hydrogen particles were estimated. Particle sizes of 1.9 mm to 8 mm (0.075 to 0.315 in.) were measured. The particle agglomerate sizes and areas were measured, and the total mass of solid hydrogen was computed. A total mass of from 0.22 to 7.9 grams of hydrogen was frozen. Compaction and expansion of the agglomerate implied that the particles remain independent particles, and can be separated and controlled. These experiment image analyses are one of the first steps toward visually characterizing these particles, and allow designers to understand what issues must be addressed in atomic propellant feed system designs for future aerospace vehicles.

NOMENCLATURE

ASTP	Advanced Space Transportation Program
DOE	Department of Energy
FCC	Face centered cubic
FOV	Field of view
GLOW	Gross lift off weight
GRC	Glenn Research Center (formerly known as Lewis)
H	Atomic hydrogen
HCP	Hexagonal close pack
H_2	Molecular Hydrogen
He	Helium
LLNL	Lawrence Livermore National Laboratory
NASA	National Aeronautics and Space Administration
NLS	National Launch System
O/F	Oxidizer to fuel ratio
SMIRF	Small Multipurpose Research Facility
STR	Space Transportation Research
USAF	United States Air Force
Wt.%	Weight percent
x/L	Non-dimensional distance from dewar lid

INTRODUCTION

For over 68 years, the promise of atomic propellants has been pursued (Refs. 1 to 10). Using atoms of boron, carbon, or hydrogen, maintained at cryogenic temperatures, very exciting advances in rocket propellants and airbreathing fuels can be created. Over the decades, many details of the physics of storing such propellants have been analyzed and experimentally determined. Current research is underway with a team from the USAF, NASA, DOE, university, industry, and small business partners (Ref. 2). The extensive data that has been amassed over the last 68 years have shown increasing storage densities for atoms in solid cryogenic storage media, and that there may be future breakthroughs that allow the more routine use of atoms for fuels.

WHY ATOMIC PROPELLANTS?

In the future, rocket and airbreathing propulsion systems may be able to gain great benefits from the enormous power of atomic propellants. A summary of atomic hydrogen rocket gross lift off weight (GLOW) is shown in Figure 1 (Ref. 3). Using a 15-wt.% atomic hydrogen fuel, the gross lift off weight of the launch vehicle can be reduced by 50 percent over the National Launch System (NLS) using O2/H2 propellants. The baseline rocket and payload weight for the comparison is an oxygen

/hydrogen rocket taking 96,000 kg of payload to Earth orbit. For the atomic hydrogen fuel, the oxidizer to fuel (O/F) ratio is 0.0. Additional analyses and suggested optimal fuel selections for atomic rocket vehicles are presented in Refs. 3 to 6, and 9.

SOLID HYDROGEN EXPERIMENTS

Solid hydrogen particle formation in liquid helium was experimentally investigated. Experiments were planned to do an initial visual characterization of the particles, observe their formation, and molecular transformations (aging) while in liquid helium. The particle sizes, molecular transformations, and agglomeration times were estimated from video image analyses (Ref. 9). The work presented here includes more detailed studies of the video images, which more precisely measured the particles sizes. In the previous work (Ref. 9), only a few of the smallest particles were analyzed. This paper's work includes the analyses of numerous images, and numerous particles in each image. The image analyses also allowed the study of the compaction or expansion of the agglomerated particles over time. Studying the compaction and expansion of the complete agglomerate will show the nature of the solid hydrogen particles, and their ability to remain independent entities. A mass estimate was not conducted in the previous work (Ref. 9). Using the new image analyses, the total mass of solid hydrogen that was formed in each run was also measured.

Characterizing solid hydrogen particles is required before any practical propellant feed system can be created. Solid hydrogen particles were selected as a means of storing atomic propellants in future launch vehicles. When storing atoms of boron, carbon, hydrogen, or other atomic materials, a solid hydrogen particle is preferred. Very low temperature ($T < 4$ K) cryogenic particles have the ability to stabilize and prevent the atoms from recombining and controlling their lifetime. The particles and the atoms must remain at this low temperature until the fuel is introduced into the engine combustion (or recombination) chamber.

EXPERIMENTAL SETUP

The experiments were conducted in the Small Multipurpose Research Facility (SMIRF, formerly the Small Multilayer Insulation Research Facility, Ref. 11). The facility has a vacuum tank, into which the experimental setup was placed. The vacuum tank is used to prevent heat leaks and subsequent boiloff of the liquid helium, and the supporting systems maintain the temperature and pressure of the liquid helium bath where the solid particles were created.

The experimental setup included several key components. Figure 2 depicts the helium dewar and the associated liquid hydrogen tank. A small cryogenic dewar was used to contain the helium bath, in which the solid hydrogen particles were formed. The dewar was 711.2 mm (28 in.) in height, with a 609.6 mm (24 in.) inside depth and had an inside diameter of 315.9 mm (12.438 in.). To create the solid hydrogen, liquid hydrogen at a temperature of 14 to 16 K was used. To contain the liquid hydrogen, a small stainless steel tank was used, which was 152.4 mm (6 in.) in diameter, and 609.6 mm (24 in.) long. As shown in Figure 2, the tank was mounted above the dewar. To control the hydrogen flow, a precision flow valve was used, and a video camera recorded the particle formation. All of the flow control for the liquid hydrogen, liquid and gaseous helium, and nitrogen purge gases was provided by the SMIRF systems.

The field of view (FOV) of the camera versus the distance from the dewar lid was computed. Figure 3 compares the camera field of view with the dewar diameter. Once the liquid helium's free surface is at $x/L = .43$ (315.9 mm, or 12.0 in., with $L = 711.2$ mm (28 in.)), the liquid's entire surface is in the FOV. For runs 1, 2, and 3, the helium liquid level was maintained at nearly 559 mm (22 in.) from the dewar lid. This location was chosen based on the knowledge of the field of view of the camera. During runs 4 to 7, the liquid level was typically at 406.4 mm (16 in.) below the lid. This height was chosen to see the particles with higher magnification, and to see if there were any specific phenomena that were not seen in the wider angle view.

Table I shows the locations of the silicon diodes for the temperature measurements. As these temperature measurements were used to establish the location of the helium surface and overall image sizes and field of view, the diode locations are presented. The detailed temperature profiles in the helium dewar are presented in Ref. 9. The diodes have a

temperature accuracy of ±1 degree K, and they are attached to a non-metallic rake, composed of circuit board material that extended from the dewar lid into the liquid helium. The diodes were mounted on the rake. Circuit board material was used as it had a low thermal conductivity, it was readily available, and was easily cut to the proper dimensions. A polycarbonate screw attached the top end of the circuit board to a polycarbonate rod. The upper end of the polycarbonate rod was threaded and screwed into the underside of the helium dewar lid.

TABLE I.—SILICON DIODE LOCATIONS IN HELIUM DEWAR
L, DEWAR = 711.2 MM (28 IN.)

Name	Location below dewar lid (in.)
SD4 (lid)	0
LL1	2
LL2	4
LL3	7
LL4	10
LL 5	12
LL 6	14
LL 7	16
LL 8	19
LL 9	22

EXPERIMENTAL PROCEDURE

During the experimental runs, a small amount of liquid hydrogen was dropped onto the surface of the liquid helium. The hydrogen flow rate selected was 1/500th liter per second, so as to see the particles form, and eliminate any chance of the relatively warm liquid hydrogen vaporizing all of the liquid helium in the dewar. A small amount of the liquid helium contained in a dewar vaporized as it froze the hydrogen particles.

In the first step of the hydrogen freezing process, the liquid hydrogen temperature was lowered to 14 to 16 K. This process allowed the hydrogen to be at a very low temperature, near its freezing point. Comparisons of the heat capacity of helium and the heats of liquefaction and fusion (solidification) of hydrogen led to the selection of conditioning the hydrogen to a very low temperature before releasing it onto the helium surface. Otherwise a large amount of helium would have been used to condense the gaseous hydrogen, liquefy it, and then finally freeze the hydrogen into solid particles. Large clouds of vapor that are created during higher speed hydrogen freezing would have also obscured the formation process, and thwarted efforts to see the final particles.

As the liquid hydrogen fell toward the helium surface, it begins to freeze and particles form immediately after hitting the helium surface. Some of the hydrogen appears to freeze as it falls, but some vaporizes as well. The hydrogen was a jet of fluid, with the outer shear layer vaporizing, but the central core remaining liquid for a short time, and finally freezing during the drop, and as it hits the helium surface.

During the fall of the hydrogen onto the helium, some of the hydrogen went into the gas phase. Small clouds of hydrogen can be seen forming about the stream of hydrogen falling onto the free surface. Additional instrumentation will be needed to assess the total mass of hydrogen that is in the gas phase versus the solid particles. The temperature profiles of the dewar may shed light on the amount of gas formed, and a thermal and mass balance analysis can be conducted to more accurately measure the distribution of hydrogen gas and solid hydrogen in the dewar. A mass spectrometer can be used to determine the mass of hydrogen in the helium gas above the liquid helium.

Solid hydrogen is less dense than helium, so the hydrogen particles floated on the surface, simplifying the particle imaging. In an operational propulsion system, this buoyancy property will be overcome by gelling the helium, thus allowing the hydrogen particles to be suspended in the helium. During the testing, it was noted that the frozen hydrogen particles may also serve as an effective gelling agent for liquid helium.

Many frames from the videotape of the experiment were captured and analyzed. Table II summarizes the timing for the experimental runs, where each solid hydrogen formation run began. There was an interval of between 25 and 65 minutes between runs. These time spans were chosen to allow the particles to

TABLE II.—SOLID HYDROGEN VIDEO EVENT TIMING

Prior to the first run, the helium level is between 19 and 22 in. below the lid.	
13:36:27	The 1st drop begins.
14:13:35	The 2nd drop begins.
14:55:02	The 3rd drop begins.
A new helium level is selected. The helium level is now between 12 and 14 in. below the lid.	
15:59:34	The 4th drop begins.
17:00:50	The 5th drop begins.
17:25:51	The 6th drop begins.
17:58:51	The 7th drop begins.

agglomerate, and to observe any unusual or unexpected properties. A more detailed listing of the events from each run and the hydrogen temperatures prior to the hydrogen release are provided in Reference 9. The small particles were allowed to float on the helium surface for at least 25 minutes before adding more hydrogen. During that 25 minute minimum time span, they began to seek each other out, agglomerate into a larger collection of particles, and minimize their surface energy as they float on the helium. The particles also turned from clear or translucent crystals to cloudy crystals, implying a transition from face centered cubic (FCC) to hexagonal close pack (HCP) molecule packing (Ref. 12). After allowing the first batch of particles to form over 3 experimental runs, we agitated the helium surface, and saw that the particles quickly broke up into their original smaller components. The particles would then again begin to agglomerate. Additional flows of liquid hydrogen were frozen on the liquid helium surface, and a larger and larger mass of particles was observed.

SOLID HYDROGEN TESTING RESULTS

Three major measurements were conducted using the solid hydrogen images: particle sizes, compaction or expansion of the complete agglomerate, and the total mass of the solid hydrogen. Appendix A contains the tabular data on particle sizes. Appendix B contains the image data of the video observations. These data are the measurements of the particle and agglomeration sizes from the video observations.

All of the observations were done with a black and white video camera, with a 56 degree field of view (or a 28 degree half angle). The lighting of the helium surface was with a fiber optic lighting system. The helium free surface was not always completely illuminated, especially for Runs 4 to 7. The indirect illumination of the reflected light from the polished dewar surfaces allowed light to illuminate the shadows surrounding the lit free surface.

Analysis Background

The images were taken with a 0.5 inch lens, charged coupled device (CCD) black and white camera. The illumination in the Dewar was created with 150 Watt bulb with the light introduced into the dewar with an optical fiber system. The VHS video images were copied to a Betacam tape format to improve the ability to obtain high definition frames for analysis. A commercially available photo manipulation and analysis software package was used.

There were three effective heights to the liquid level that were used in the image analyses. The highest level for the helium was during Runs 4 and 5 (x/L = 0.5, 14 in. below the lid), the lowest in runs 1 to 3 (x/L = 0.786, 22 in. below the lid), and in the intermediate height during runs 6 and 7 5 (x/L = 0.571, 16 in. below the lid). Three different baseline sizes for the overall image area (representing the entire free surface helium in the dewar) were used. The specific particle sizes were then measured, and the ratio of the two, with the overall dewar surface area, is used to compute the particle size.

Particle sizes

The solid hydrogen particles were analyzed by digitizing the video images, and measuring the sizes of the particles. The particle size measurements were corrected for the actual size of the particles using these equations:

area, particle = (area, dewar/pixels, dewar) x pixels, particle

where:

area, particle = area of the particle (mm^2)
area, dewar = area of the dewar free surface (mm^2)

pixels, dewar = number of pixels in the imaged free surface
pixels, particle = number of pixels in the imaged particle

At the beginning of and during each run, a variety of individual particles are measured. The smallest of the particles is identified, as well as a representative set of other larger particle sizes. Figure 4 illustrates a typical image from the analyses. The circle encompasses a small set of hydrogen particles that have agglomerated.

Figures 5 and 6 provide the particle sizes. Overall, the initial formed particles were 1.9 mm to 8 mm (0.075 to 0.315 in.) in diameter. These particles were the smallest particles that formed during the initial freezing of the hydrogen. In this testing, no control was placed on the particle formation, other than the helium and hydrogen temperature and pressure and the flow rate of the hydrogen. The simple freezing process is somewhat random, and the particles will vary in size simply due to the random breakup of the stream of hydrogen that fell onto the helium during the freezing process. The other measurement variation of the particles from the video images that occurred was that all of the particles were not perfectly spherical or elliptical, thus an effective circular diameter, based on the particle area was calculated. These initial particle sizes were later used to estimate the thickness of the hydrogen layer that formed on the helium surface.

Compaction and Expansion of Particle Agglomerations

Compaction and expansion: After the particles have agglomerated, the overall agglomerate tends to begin compacting and expanding. The agglomerate is composed of many millimeter sized particles. Figure 7 compares two images from Run 7, and shows the subtler changes of size of the agglomerate. The compaction and expansion of the agglomerate was evident after detailed sizing analyses were performed. Figure 8 shows this particle diameter comparison, and the sudden change in area that occurs later in the run.

At the end of Run 7, the particles that had compacted were agitated to break up the agglomerate. The newly formed particles tended to cover a much greater area, and almost formed a gel structure across the liquid helium surface. Figure 9 compares the particle agglomerate shape from the time of 17,330 seconds (18:25:17) to 17,676 seconds (18:31:03) and shows this new expanded structure. This new more filamentous structure for the particles persisted until the end of the run. The earlier image is during the quiescent agglomeration period, and the later image shows the result of the violent break up of the particles caused by lowering the dewar pressure. The effective agglomerate diameter increased from 118.7 mm to 139.1 mm. This showed that the particles will break up into their smaller original constituents, and are largely able to remain independent entities.

Total mass of solid hydrogen: After freezing occurs, and all of the particles have agglomerated at the end of each run, the total mass of hydrogen is calculated. The calculation is conducted by measuring the total area of the hydrogen agglomerate, multiplying by its thickness, and finally multiplying by the density of the solid hydrogen.

Mass = area x thickness x density

where:

Mass = total mass of solid hydrogen (g)
area = area of solid hydrogen agglomerate (mm^2)
thickness = thickness of solid hydrogen agglomerate (mm)
density = density of solid hydrogen (g/mm^3)

The thickness of the hydrogen layer was estimated based on the observed diameters smallest particles that were observed during the beginning of an individual run. Figure 10 illustrates the assumptions about the hydrogen layer thickness. The smallest diameter particles were measured during the first few minutes of the run. The largest and smallest individual particles that were found during the beginning of the run were used as the thickness of the hydrogen layer. In observing the solid hydrogen, it was found that the particles tended to agglomerate after the initial freezing process, but the particles were easily distinguished as separate entities during the agglomeration process. The density of helium and hydrogen are sufficiently different that all of the hydrogen

particles float on the helium surface. No large "icebergs" of hydrogen are created in the freezing process.

Two densities were used for the solid hydrogen: 7.7×10^{-5} and 9.0×10^{-5} g/mm^3 (77 and 90 kg/m^3). These data were obtained from Refs. 13 to 16. A variation in the density was considered, as some of the particles may not be of a uniform density. Also, the density of the solid hydrogen may increase with time (Ref. 14) with longer exposure to cryogenic temperatures.

The planned flow rate of liquid hydrogen was 1/500th liter per second, or 0.154 g/s. On runs 1 to 6 the on-time for the liquid hydrogen valve was 7 to 13 seconds (Ref. 9), but only 1 to 3 seconds of flow was observed. Using the total mass data and the timing for each run, the average mass flow rate can be estimated. The average flow rate for Run 1 was from

Mass flow rate (g/s) = 0.220 g/3 s =
= 0.073 g/s (for H2 density, 77 kg/m^3)

to:

Mass flow rate (g/s) = 0.421 g/3 s =
= 0.1403 g/s (for H2 density, 90 kg/m^3)

Thus, the flow rates have a good match to the observed and desired flow rates.

Figures 11 and 12(a) and (b) show the total masses of hydrogen calculated from the image analyses. Runs 1 to 3 (in Figure 11) and Runs 4 to 7 (in Figures 12(a) and (b)) are contiguous runs, and these are presented in separate figures. The figures present a matrix of sizes from each run, as the precise hydrogen density and particle size (and the hydrogen layer thickness) is not known. Run 1 produced about 0.22 to 0.421 grams of solid hydrogen. By Run 3, the total mass of solid hydrogen produced 1.6 to 3.6 grams. At the end of Run 7, the total mass of hydrogen was 2.34 to 7.9 grams.

The variation in particle size, and therefore the thickness of the hydrogen layer is especially interesting for Runs 1 to 3. Larger particles were formed in Run 1, but smaller particles were able to form in Runs 2 and 3. In Runs 4 to 7, the particles did tend to be larger as time progressed, and this may be due to some clumping of the solid hydrogen as time proceeds.

OBSERVATIONS

Precise knowledge of the hydrogen layer thickness was difficult to achieve. The particle sizes of the hydrogen were somewhat random. The variation in the solid hydrogen mass estimate was due to the uncertainties in the thickness of the hydrogen layer and the hydrogen density. More precise knowledge of the hydrogen density over time is needed. Additional higher resolution imaging of the hydrogen on the surface and at the surface level can provide important information to solve this difficulty.

As the particles were agglomerating, some of the particles tend to stick together more tenaciously, and others rolled in the liquid helium, and only lightly osculated with the other large agglomeration. Sometimes, this motion persisted, and the area of the agglomerate varied from minute to minute, making a perfect measurement more difficult.

Breaking up the particles was typically easy to accomplish. The pressure was reduced in the dewar to several psi less than atmospheric pressure, and the particles readily dispersed. Once the vacuum was turned on, and the particles were forced to separate, we saw the larger agglomerates or clumps, and some of these particle clumps persisted in a larger size.

The small area that creates nucleate boiling will make the particle move in random motions, and prevent a quick agglomeration if there is only a small mass of hydrogen on the surface.

There is a bright spot in the middle of the image for only the initial Runs 1 to 3. There was a localized nucleation site at the bottom of the dewar, that created a miniature boiling bubble stream, looking like a "tornado," which reflected light directly back to the camera. During Runs 4 to 7, when the surface was quiescent, the reflected light appeared due to the polished dewar surfaces.

In some cases, there seemed to be a cloud of hydrogen or helium above the liquid free surface, which complicated the image analyses. These clouds took on two distinct forms. The first was simply a cloud of hydrogen that occurred because of the high flow rate into the dewar. This cloud dissipates as the hydrogen temperature drops, and the gas freezes, or goes

up the vent from the dewar. The second cloud is more fascinating, as it persists above the helium surface, but only under some specialized and, at least with this testing, mostly unreproducible conditions.

A sheen or brightening of the hydrogen surface occurs when additional hydrogen is dropped directly onto the preexisting solid hydrogen from a previous run. This brightening is likely to be very tiny particles that have formed on the preexisting solid hydrogen, depositing from the gas phase. Such tiny particles were rarely seen, but their effect may be important and must be accounted for in future experimental planning.

In the formation of the solid hydrogen particles, there were several rules of thumb that allowed better visualization of the surface. The quiescent surface of the helium allowed for the best visualization. Any contamination of the dewar surface created nucleating sites, which led to bubbles that can reflect light and obscure the particles. Subsequent testing in 2001 used a small aluminum cone to diffuse the light from the optical fiber system, preventing any further glare or reflections.

The mass flow rate of liquid hydrogen to form solid hydrogen must be small enough to prevent clouding of the field of dewar during a run. These clouds are vaporizing hydrogen, and the vapor may lead to inefficient hydrogen production. A continuous flow process where the hydrogen is carried away from the liquid hydrogen drop zone would likely be a good engineering solution and make for an efficient future production scheme.

New testing that was recently completed in 2001 showed other ways to create very tiny solid particles, with condensation of hydrogen gas. This formation process however, may be much more costly (much more helium required to freeze gaseous hydrogen) than using liquid hydrogen. In the subsequent solid hydrogen testing conducted in 2001, it appeared that tiny particles were observed freezing on the walls, and then slumping into the liquid helium. In other cases, the tiny particles appeared to scintillate, and in some cases appear to be microscopic. The particle created chains and "concatenated" into strings, and curled up into tight balls of solid hydrogen. Analyses of these data will no doubt find more preferred solutions for particle production.

CONCLUSIONS

Using video images from hydrogen freezing experiments, solid hydrogen particle sizes and the total masses of solid hydrogen were measured. The smallest particle sizes found in the experiments were from 1.9 to 8 mm (0.075 to 0.315 in.) in diameter. After allowing the particles to agglomerate, the new complete agglomerate is typically a loose collection of the smaller particles, and is easily dispersed.

Compaction and expansion of the agglomerate implied that the particles remain independent particles, and can be separated and controlled. At the end of Run 7, the particles that had compacted were agitated to break up the agglomerate. The newly formed particles tended to cover a much greater area, and almost formed a gel structure across the liquid helium surface. This new more filamentous structure for the particles persisted until the end of the run. The effective agglomerate diameter increased from 118.7 mm to 139.1 mm. This showed that the particles will break up into their smaller original constituents, and are largely able to remain independent entities.

The total masses of solid hydrogen created were from 0.22 to 7.9 grams. The data presents a matrix of sizes from each run, as the precise hydrogen density and particle size (and the hydrogen layer thickness) is not known. Run 1 produced about 0.22 to 0.421 grams of solid hydrogen. By Run 3, the total mass of solid hydrogen produced 1.6 to 3.6 grams. At the end of Run 7, the total mass of hydrogen was 2.34 to 7.9 grams.

CONCLUDING REMARKS

Many researchers have investigated the formation of solid hydrogen particles. Additional research conducted with solid hydrogen (Refs. 17 to 32) has pointed to many ways of creating particles that are acceptable for fusion energy research, and many other applications. The precise control of the formation process will be needed for storing atomic species in the solid hydrogen particles.

The formation and size of the particles in this testing were not controlled, save for the control of temperature and pressure. However, the size variations of the smallest particles seem to fall within the needed size for solid particle feed systems: 1.9 to 8 mm (0.075 to 0.315 in.) diameters. This observation bodes well for lower cost hydrogen particle production.

Solid hydrogen and atomic propellants have a possible future not only for rocket propellants, but energy storage on Earth as well as systems to assist Humankind's efforts to explore and one day establish human bases and more permanent footholds in the Outer Solar System. Of course, our current abilities to store atoms in solid hydrogen are limited with only a fraction of 0.1 wt.% being stored. For effective propulsion, we must have from 15- and 50-wt.% of stored atoms. Hopefully with time, our abilities to manipulate matter and understand the basic nature of atomic species will catch up with our propulsion visions and imaginations, and make possible the fantastic potential for atomic rocket propellants.

REFERENCES

1) Palaszewski, B., "Atomic Hydrogen Propellants: Historical Perspectives and Future Possibilities," NASA Lewis Research Center, AIAA–93–0244, NASA TM–106053, presented at the 31st AIAA Aerospace Science Meeting, Reno, NV, January 11–14, 1993.

2) Palaszewski, B., Ianovski, L., and Carrick, P., "Propellant Technologies: Far Reaching Benefits for Aeronautical and Space Vehicle Propulsion," in the Special Edition of the AIAA Journal of Propulsion and Power, September/October 1998, pp. 641–648.

3) Palaszewski, B., "Launch Vehicle Performance for Bipropellant Propulsion using Atomic Propellants with Oxygen," NASA Glenn Research Center at Lewis Field, AIAA–99–2837, presented at the 35th AIAA/ASME/SAE Joint Propulsion Conference, Los Angeles, CA, June 1999.

4) Palaszewski, B., "Launch Vehicle Performance with Solid Particle Feed Systems for Atomic Propellants," AIAA–98–3736, NASA/TM—1998-208498, presented at the 34th AIAA/ASME/SAE Joint Propulsion Conference, Cleveland, OH, July 1998.

5) Palaszewski, B., "Solid Hydrogen Testing And Analyses For Atomic Rocket Propulsion," presented to the Propulsion Engineering Research Center (PERC) 11th Annual Symposium on Propulsion, The Atherton Hotel, State College, PA, November 18–19, 1999.

6) Palaszewski, B., "Atomic Propellants for Aerospace Propulsion Systems: Solid Hydrogen Experiments and Vehicle Analyses," presented at the 1999 USAF High Energy Density Materials Contractors Conference, Cocoa Beach, FL, June 8–10, 1999.

7) Palaszewski, B., "Atomic Hydrogen As A Launch Vehicle Propellant," NASA Lewis Research Center, AIAA–90–0715, NASA TM–102459, presented at the 28th AIAA Aerospace Science Meeting, Reno, NV, January 8–11, 1990.

8) Lubell, M., Lue, J., and Palaszewski, B., "Large-Bore Superconducting Magnets for High Energy Density Propellant Storage," presented at the 1996 Applied Superconductivity Conference, Pittsburgh, PA, August 25–30, 1996.

9) Palaszewski, B., "Solid Hydrogen Experiments for Atomic Propellants," NASA Glenn Research Center at Lewis Field, AIAA–2000–3855, presented at the 36th AIAA/ASME/SAE Joint Propulsion Conference, Huntsville, AL, July 2000.

10) Sanger, E., Rocket Flight Engineering, NASA Technical Translation, NASA TT–F–223, Translation Into English of the book "Raketenflugtechnik" Berlin, Verlag Von Oldenburg, 1933, translation published September 1, 1965.

11) Dempsey, P., and Stochl, R., "Supplemental Multilayer Insulation Research Facility," NASA Lewis Research Center, NASA TM–106991, July 1995.

12) Silvera, I., "The Solid Molecular Hydrogens in the Condensed Phase: Fundamentals and Static Properties," Reviews of Modern Physics, Vol. 52, No. 2, Part I, April 1980, pp. 393–452.

13) McCarty, R.D., "Hydrogen Technology Survey: Thermophysical Properties," National Bureau of Standards, NASA Technical Reports, NASA–SP–3089, January 1975.

14) Fajardo, Mario, USAF Research Laboratory, Edwards, CA, personal communication, July 1999.

15) McNellis, N., et al., "A Summary Of The Slush Hydrogen Technology Program For The National Aero-Space Plane," NASA/TM–106863, AIAA–95–6056, presented at the Hypersonics Technologies Conference, Chattanooga, TN, Apr. 3–7, 1995.

16) Hardy, T.L., "FLUSH: A Tool for the Design of Slush Hydrogen Flow Systems," Technical Memorandum, NASA/TM–102467, Lewis Research Center, Feb. 1, 1990.

17) Sater, J.D., Pipes, J., and Collins, G.W. "Cryogenic D-T Fuel Layers Formed In 1-mm Spheres By Beta-Layering," Report Number UCRL–JC–128031–ABS–REV–1, Lawrence Livermore National Laboratory, Target Fabrication Meeting '98, 1998.

18) Collins, G.W., Sanchez, J.J., Bernat, T., Sater, J.D., and Bittner, D., Forming Uniform D-T And D2 Layers For Cryogenic NIF Targets," Report Number UCRL–JC–129969–ABS, Lawrence Livermore National Laboratory, European Conference on Laser Interaction with Matter, 1998

19) Bittner, D.N., Collins, G.W., Monsler, E., and Letts, S., "Forming Uniform HD Layers In Shells Using Infrared Radiation," Livermore National Laboratory, Report Number UCRL–JC–131371, 40th Annual Meeting of the Division of Plasma Physics, New Orleans, LA, November 16–20, 1998.

20) Collins, G.W., Bittner, D.N., Monsler, E., Letts, S., Tiszauer, D., Feit, M., Mapoles, E.R., and Bernat, T.P., "Forming And Smoothing D2 and HD Layers For ICF By Infrared Heating," Lawrence Livermore National Laboratory, Report Number UCRL–JC–123596–ABS, European Conference on Laser Interaction with Matter, 24th, Madrid, Spain, June 3–7, 1996

21) Collins, G.W., Mapoles, E.R., Sanchez, J.J., Bernat, T., Sater, J.D., Bittner, D., Sheliak, J.D., Hoffer, J.K., "Reducing DT Surface Roughness For Cryogenic Ignition Targets," Lawrence Livermore National Laboratory, Report Number UCRL–JC–124884–ABS, Annual Meeting of the American Physical Society Division of Plasma Physics, 38th, Denver, CO, November 11–15, 1996.

22) Kozioziemski, B. J., Collins, G.W., and Bernat, T.P., "Single Crystal Growth of Solid D2," Lawrence Livermore National Laboratory, Report Number UCRL–JC–125981–ABS, 1997 March Meeting of the American Physical Society, Kansas City, MO, March 17–21, 1997, 1996.

23) Kozioziemski, B.J., Collins, G.W., Bernat, T.P., Mapoles, E.R., and Unites, W., "Crystal Growth And Roughening Of Solid D2," Lawrence Livermore National Laboratory, Target Fabrication Specialist's Meeting, 11th, Orcas Island, WA, September 8–12, 1996, Report Number UCRL–JC–125121–ABS, Fusion Technology, Vol. 31, pp. 482–484, July 1997

24) Bittner, D.N., Collins, G.W., Letts, S., and Monsler, E., "Generation Of Uniform Solid HD Layers Inside Spherical Capsules Using Infrared Illumination," Lawrence Livermore National Laboratory, Report Number UCRL–JC–125140–ABS, Conference, Target Fabrication Specialist's Meeting, 11th, Orcas Island, WA, September 8–12, 1996.

25) Bernat, T.P., Collins, G.W., Mapoles, E.R., and Duriez, C., "Heat-Flux Induced Changes To Multicrystalline D2 Surfaces," Lawrence Livermore National Laboratory, Report Number UCRL–JC–124261–ABS–REV–1, 39th Annual Meeting of the APS (American Physical Society)/DPP (Division of Plasma Physics), Pittsburgh, PA, November 17–21, 1997.

26) Kozioziemski, B.J., Collins, G.W., and Bernat, T.P., "D2 Crystal Growth and Surface Energy," Lawrence Livermore National Laboratory, Report Number UCRL–JC–130037–ABS, Target Fabrication Meeting '98, Jackson Hole, Wyoming, April 19–23, 1998.

27) Fajardo, M., "Cryosolid Propellants—The Last "Revolutionary" HEDM Concept," in Berman, M. (editor), Proceedings of the High Energy Density Matter (HEDM) Contractors Conference, Scientific Special, June 8–10, 1999, January 2000.

28) Larson, C.W., "Kinetics of Boron Carbon HEDM," in Berman, M. (editor), Proceedings of the High Energy Density Matter (HEDM) Contractors Conference, Scientific Special, June 8–10, 1999, January 2000.

29) Talroze, V.L., Gordon, E.B., Ivanov, B.I., Perminov, A.P., Ponomarev, A.N., "Measurement Of The Hyperfine State Of The Hydrogen Atom As It Interacts In The Gas Phase With CO, SO2, CO2 And N2O Molecules," Akademiia Nauk SSSR Page: vol. 227, Akademiia Nauk SSSR, Doklady, vol. 227, Mar. 11, 1976, p. 407–410. In Russian. Mar. 11, 1976, pp. 407–410. In Russian.

30) Gordon, E.B., Perminov, A.P., Ivanov, B.I., Matiushenko, V.I., Ponomarev, A.N., and Tal'roze, V.L., "Change In The Hyperfine State Of The Hydrogen Atom During Its Collisions With Unsaturated Hydrocarbon Molecules In The Gaseous State," (Previously cited in issue 23, pp. 3317, (Zhurnal Eksperimental'noi i Teoreticheskoi Fiziki, vol. 63, Aug. 1972, pp. 401–406.) Soviet Physics – JETP, vol. 36, Feb. 1973, pp. 212–215. Translation.

31) Hardy, W.N., Klump, K.N., Schnepp, O., Silvera, I.F. "Optical Phonons In Solid Hydrogen And Deuterium In The Ordered State," Phys. Rev. Letters, Vol. 21, No. 5, July 29, 1968. pp. 291–294.

32) Agosta, C.C., Silvera, I.F, Stoof, H.T.C., and Verhaar, B.J., "Trapping Of Neutral Atoms With Resonant Microwave Radiation," Technische Univ., Few-Body Collisions in a Weakly Interacting Bose Gas," reprinted from Physical Review Letters (American Physical Society), v. 62, no. 20, 15 May 1989 pp. 2361–2364.

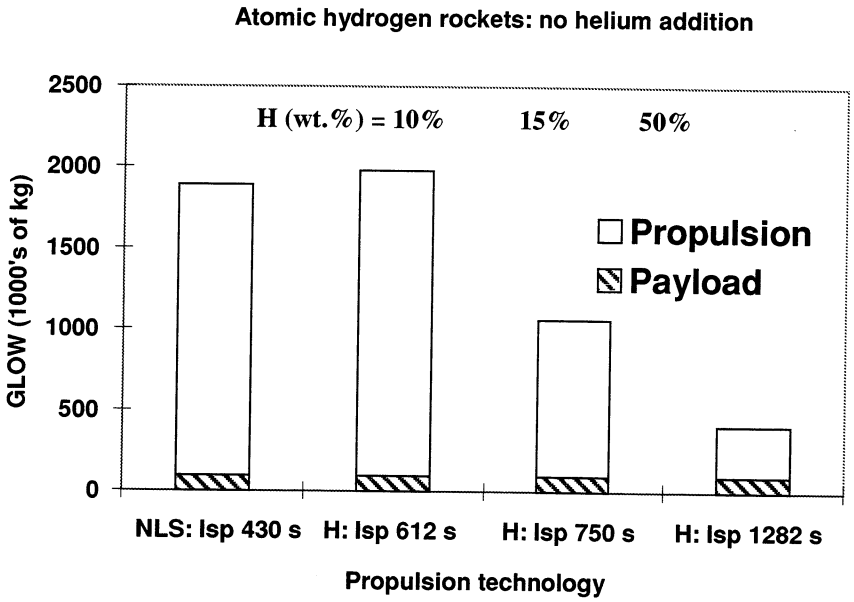

Figure 1.—Atomic hydrogen GLOW for monopropellants: 10-, 15, and 50-wt.% H, NLS = National Launch System, 96,000 kg payload for all vehicles.

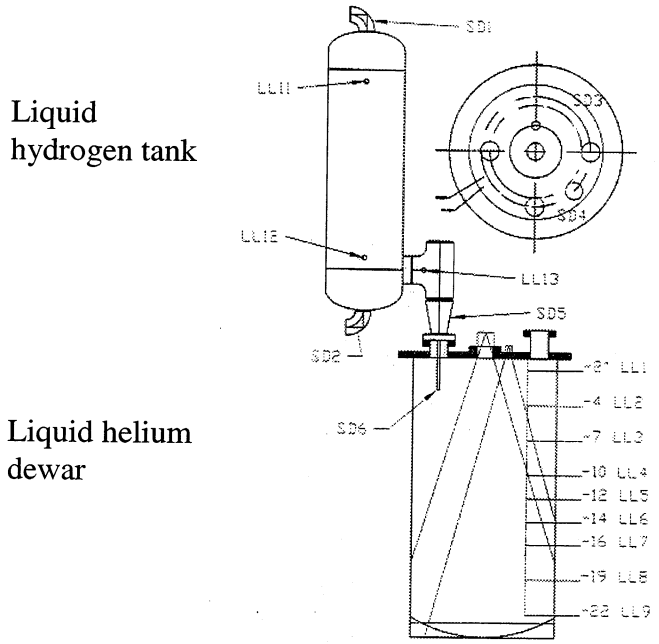

Figure 2.—Solid hydrogen testing: helium dewar and liquid hydrogen tank arrangement.

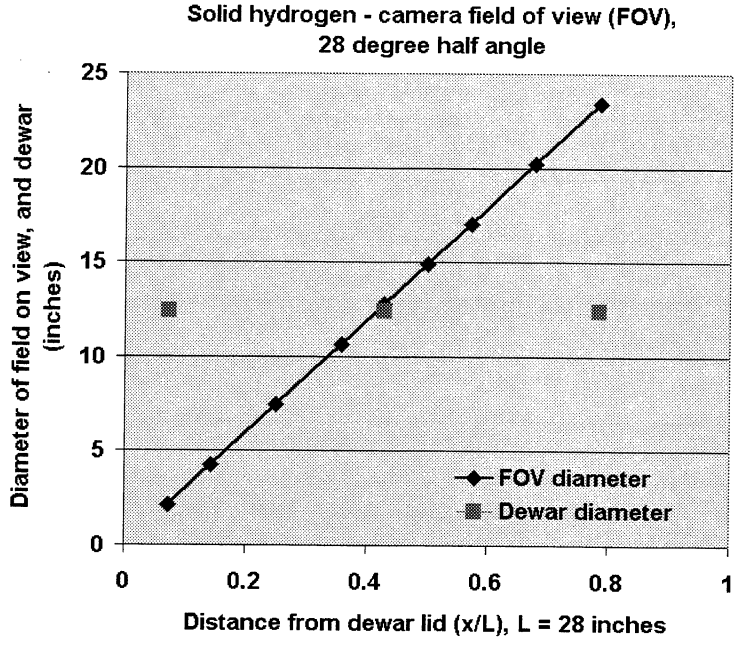

Figure 3.—Solid hydrogen experiment: camera field of view (FOV), dewar diameter = 315.9 mm.

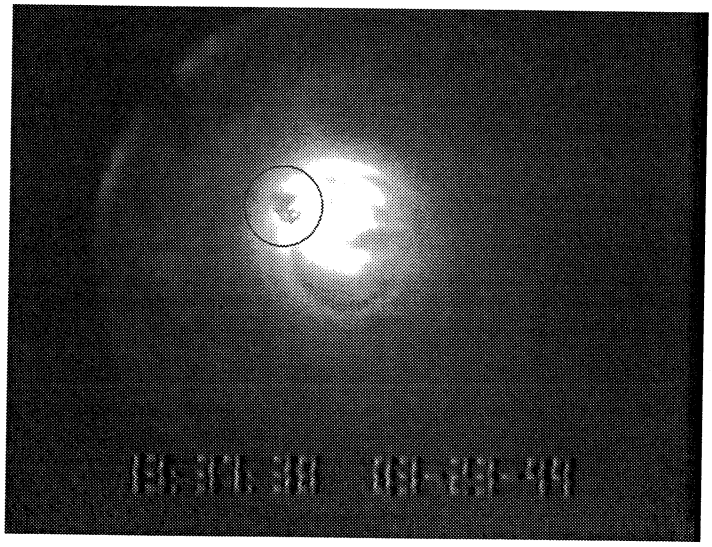

The circle contains a representative partial agglomeration of solid hydrogen particles.

Figure 4.—Solid hydrogen particle formation experiment: Run 1, at 13:37:38.

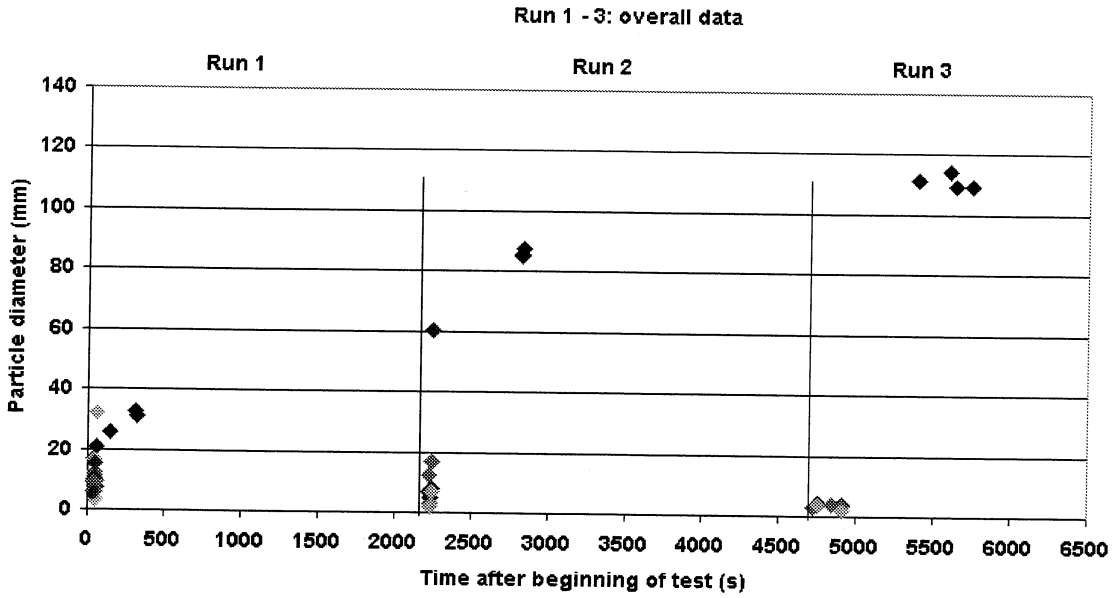

Figure 5.—Solid hydrogen particle diameters: Run 1 to 3 – 3/23/1999.

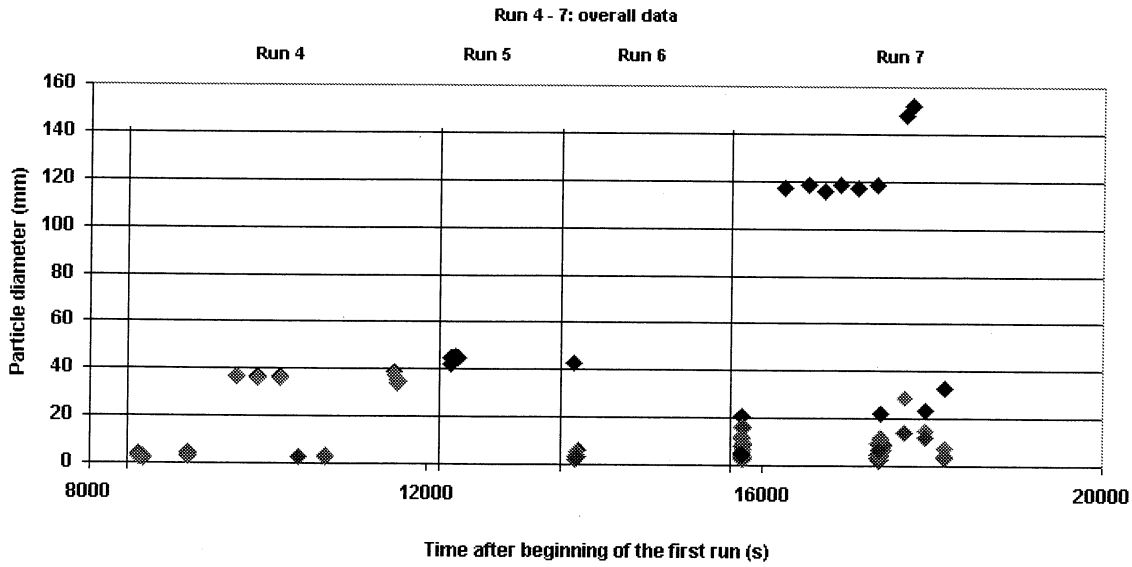

Figure 6.—Solid hydrogen particle diameters: Runs 4 to 7 – 3/23/1999.

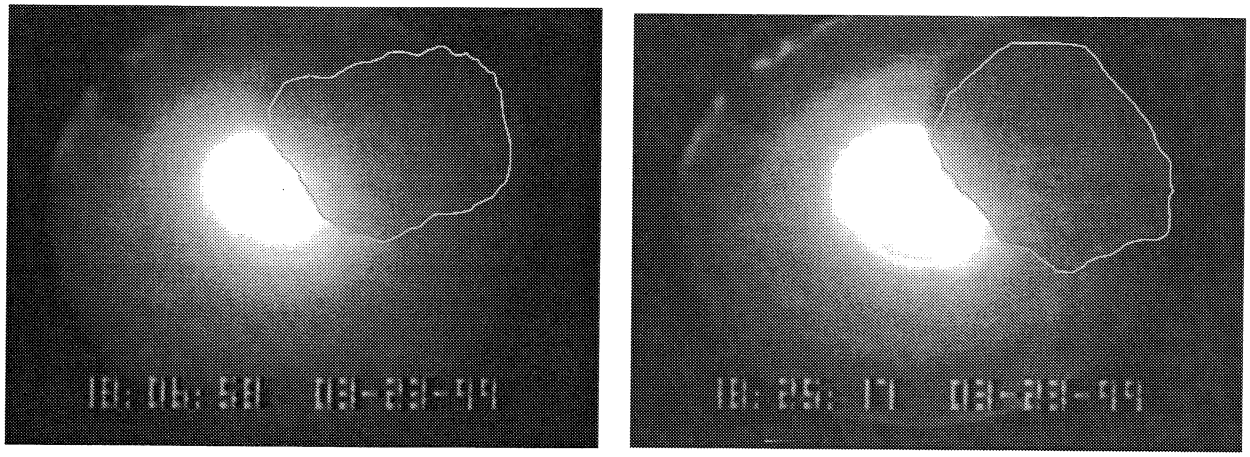

Figure 7.—Solid hydrogen particle agglomerate compaction – expansion example: Runs 7 – at 16,231 seconds (18:06:58) and 17,330 seconds (18:25:17).

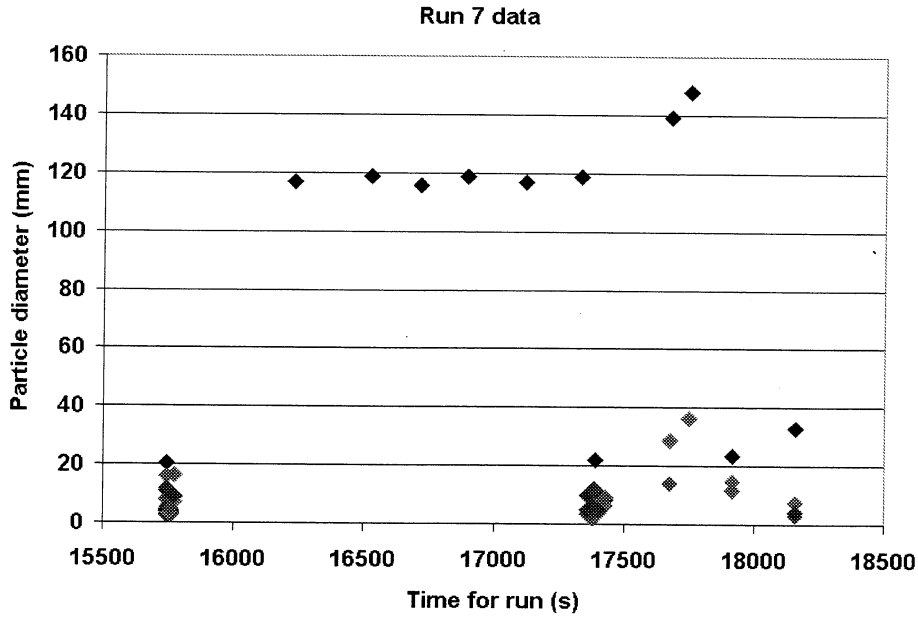

Figure 8.—Solid hydrogen particle diameters: Runs 7 – 3/23/1999.

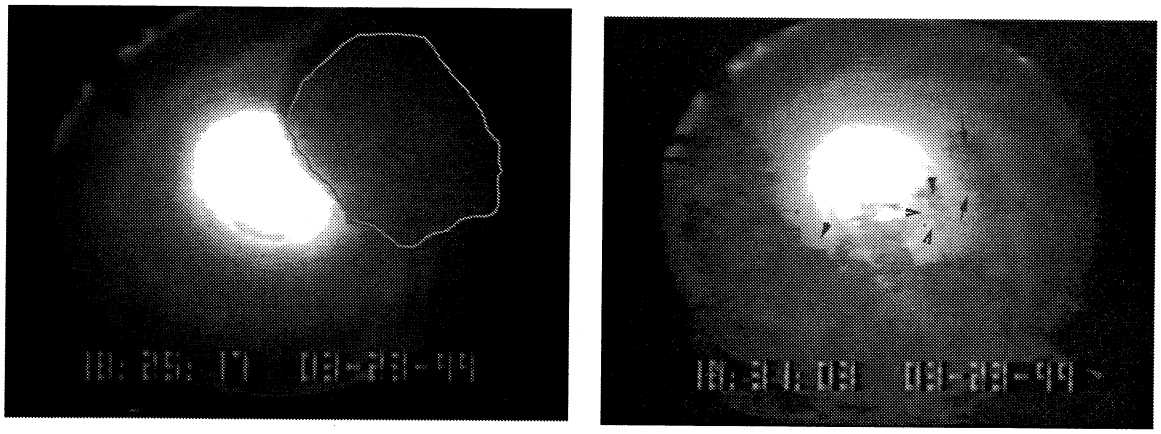

Figure 9.—Solid hydrogen particle agglomerate compaction – expansion example: Runs 7 – at 17,330 seconds (18:25:17) and 17, 676 seconds (18:31:03).

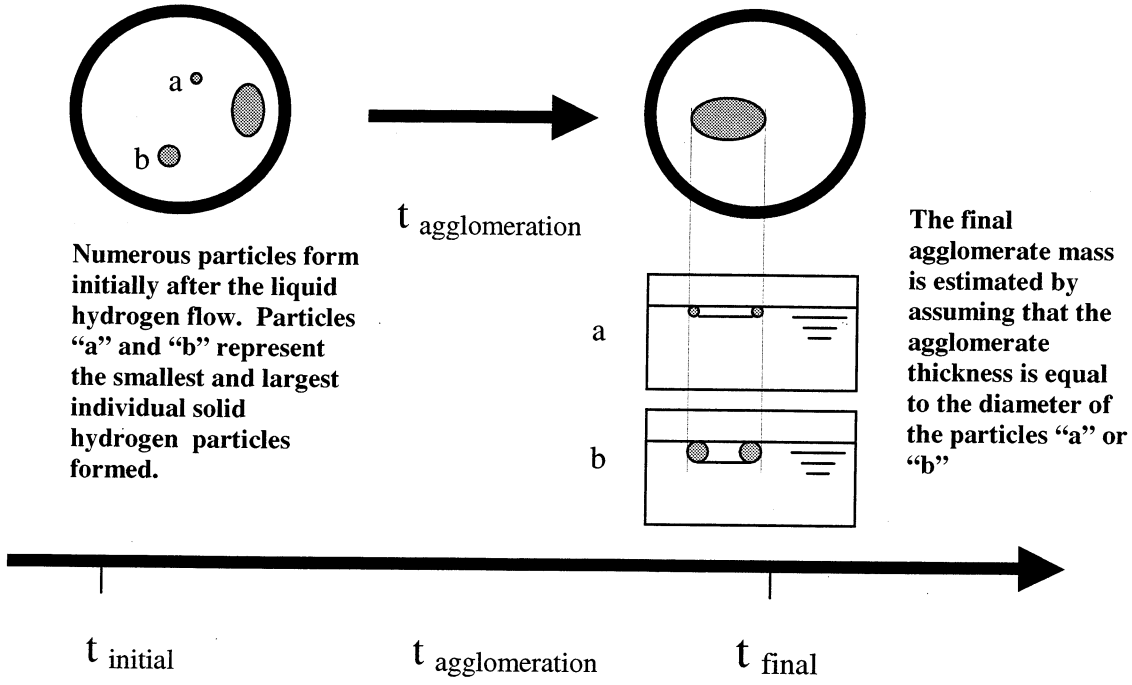

Figure 10.—Solid hydrogen mass estimation – illustration.

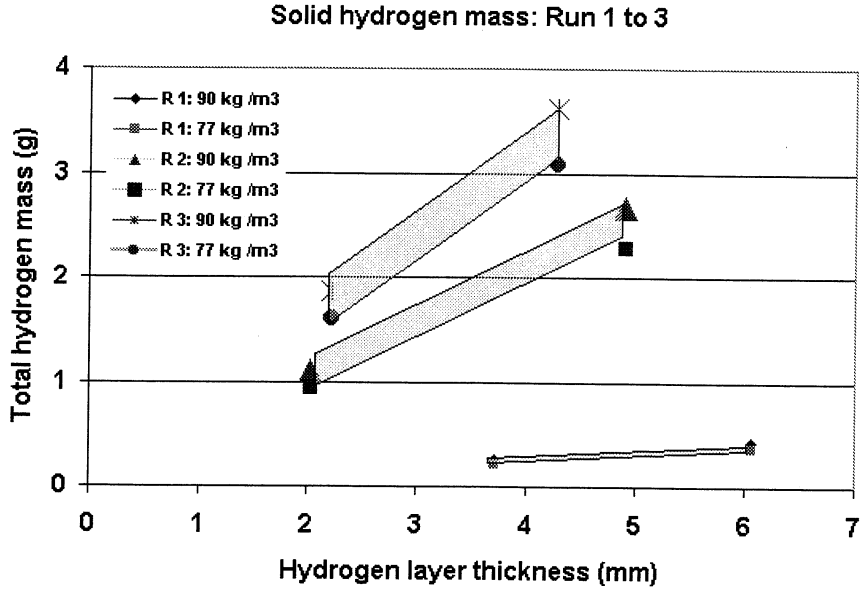

Figure 11.—Total mass of solid hydrogen: Runs 1 to 3.

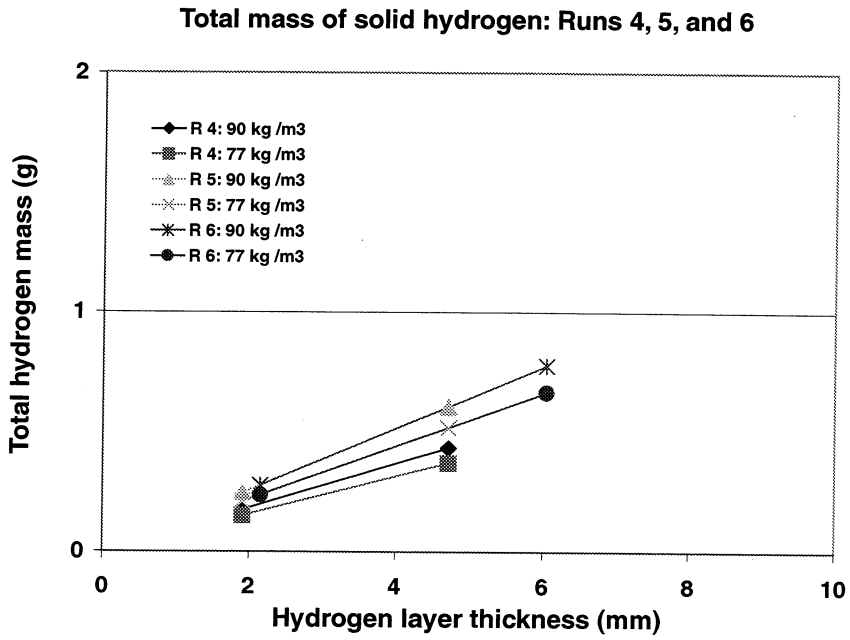

(a)

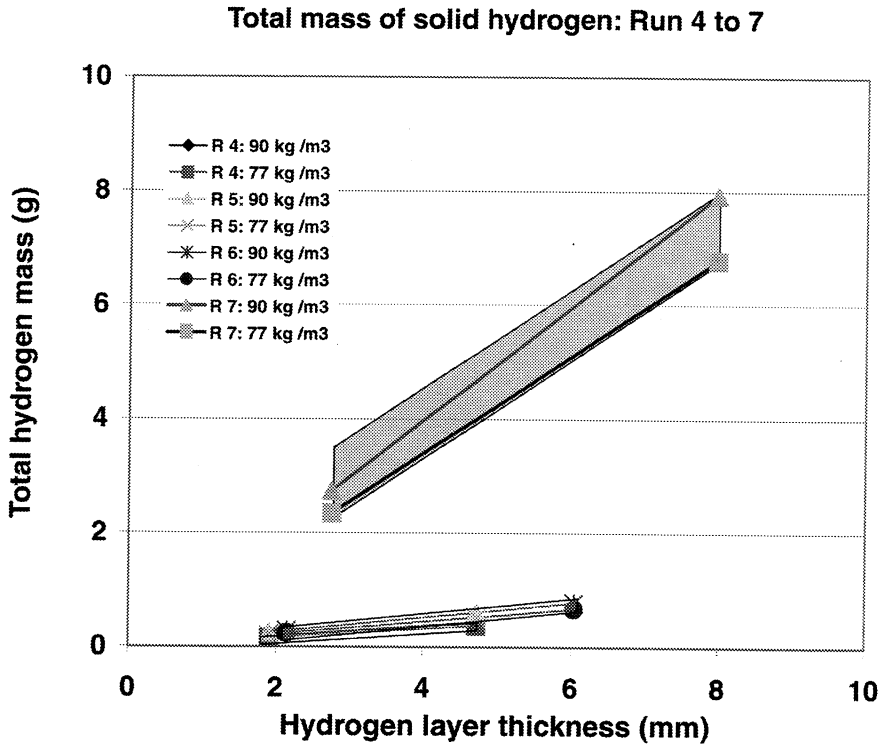

(b)

Figure 12.—(a) Total mass of solid hydrogen: Runs 4 to 6. (b) Total mass of solid hydrogen: Runs 4 to 7.

Appendix A: Solid Hydrogen Experiments for Atomic Propellants
Data from image analyses

Bryan Palaszewski
NASA Glenn, MS 5-10
05/30/2001

Solid Hydrogen Experiments for Atomic Propellants

Particle sizes from Solid Hydrogen video observations

Dewar Diameter = 12.4375 in.

Dewar inside diameter = 12 and 7/16 inches

Particle size calibrations
Run 1-3 at 72 dpi. = 508,664 pixels
Run 4-5 at 72 dpi. = 538,483 pixels
Run 6-7 at 72 dpi. = 541,063 pixels

				t within run	t overall	a	b	c	d	e	f
Run 1	time										
	13:36:27			0.0	0.0						
Particle diameter (mm)	**13:37:06**	0:00:39	0:00:39	**39.0**	**39.0**	6.057203	16.59129	9.602843	9.78499	9.001711	4.248577
	13:37:15	0:00:48	0:00:48	**48.0**	**48.0**	11.31033	11.14431	3.705953	15.21568	6.688326	6.024701
	13:37:18	0:00:51	0:00:51	**51.0**	**51.0**	7.29182	12.57531	16.42488	10.31217	6.008401	
	13:37:25	0:00:58	0:00:58	**58.0**	**58.0**	20.86556					
	13:37:28	0:01:01	0:01:01	**61.0**	**61.0**	7.62074	9.343967	32.18908			
	13:38:54	0:02:27	0:02:27	**147.0**	**147.0**	25.50311					
	13:41:44	0:05:17	0:05:17	**317.0**	**317.0**	32.77206					
	13:41:46	0:05:19	0:05:19	**319.0**	**319.0**	31.35236					
Run 2											
Particle diameter (mm)	14:13:35		0:37:08	0.0							
	14:13:34		0:37:07	0.0	2227.0	6.717617	12.2513				
	14:13:39	0:00:04	0:37:12	5.0	2232.0	4.77068					
	14:13:42	0:00:07	0:37:15	8.0	2235.0	4.972063	2.938175	2.029834			
	14:13:48	0:00:13	0:37:21	14.0	2241.0	7.973038	17.06351	6.688339	60.48271		
	14:23:32	0:09:57	0:47:05	598.0	2825.0	85.36006					
	14:23:35	0:10:00	0:47:08	601.0	2828.0	85.0884					
	14:23:43	0:10:08	0:47:16	609.0	2836.0	87.77162					
Run 3											
Particle diameter (mm)	**14:55:02**		1:18:35	0.0	4715.0						
	14:55:17	0:00:15	1:18:50	15	4730.0	2.870622	3.068824				
	14:55:45	0:00:43	1:19:18	43	4758.0	4.294526	4.178749	4.083761			
	14:57:14	0:02:12	1:20:47	132	4847.0	3.961834	3.758526				
	14:58:15	0:03:13	1:21:48	193	4908.0	4.059672	3.598515	2.214731			
	15:06:21	0:11:19	1:29:54	679	5394.0	111.2916					
	15:09:44	0:14:42	1:33:17	882	5597.0	114.3017					
	15:10:25	0:15:23	1:33:58	923	5638.0	109.4437					
	15:12:11	0:17:09	1:35:44	1029	5744.0	109.1367					

Appendix A: Solid Hydrogen Experiments for Atomic Propellants
Data from image analyses

Bryan Palaszewski
NASA Glenn, MS 5-10
05/30/2001

Solid Hydrogen Experiments for Atomic Propellants

Particle sizes from Solid Hydrogen video observations

Dewar Diameter = 12.4375 in.

Dewar inside diameter = 12 and 7/16 inches

Particle size calibrations
Run 1-3 at 72 dpi. = 508,664 pixels
Run 4-5 at 72 dpi. = 538,483 pixels
Run 6-7 at 72 dpi. = 541,063 pixels

	time					a	b	c	d	e	f	g	h	I
Run 4														
Particle diameter (mm)	**15:59:34**		2:23:07	0.0	8587.0									
	15:59:44	0:00:10	2:23:17	10	8597.0	2.583046	2.558578	2.696979						
	16:00:29	0:00:55	2:24:02	55	8642.0	2.618675	2.593871	1.907052	2.215794					
	16:08:19	0:08:45	2:31:52	525.0	8587.0	4.106781	4.067881	3.88496	4.156323	3.247592	3.593161	2.763581		
	16:09:14	0:09:40	2:32:47	580.0	9167.0	4.755112	4.710071	4.199846	3.191108	2.985008				
	16:11:33	0:11:59	2:35:06	719.0	9306.0									
	16:18:39	0:19:05	2:42:12	1145.0	9732.0	36.85054	36.50149							
	16:22:54	0:23:20	2:46:27	525.0	9987.0	36.49171	36.14605							
	16:27:20	0:27:46	2:50:53	1666.0	10253.0	36.67409	36.32671							
	16:31:09	0:31:35	2:54:42	1895.0	10482.0	2.473078	2.449652	2.663053	2.730483	2.860578	2.828615			
	16:36:15	0:36:41	2:59:48	2201.0	10788.0	3.134143	3.104455	2.828615	3.618376					
	16:50:02	0:50:28	3:13:35	3028.0	11615.0	38.76242	37.39232							
	16:50:25	0:50:51	3:13:58	3051.0	11638.0	35.64124	34.00761							
	16:50:46	0:51:12	3:14:19	3072.0	11659.0	34.91626	34.58553							
Run 5							36.05791							
Particle diameter (mm)	**17:00:50**		3:24:23	0.0	12263.0									
	17:01:22	0:00:32	3:24:55	32	12295.0	44.704								
	17:01:25	0:00:35	3:24:58	35	12298.0	42.04606								
	17:01:38	0:00:48	3:25:11	48.0	12311.0	44.94013								
	17:02:02	0:01:12	3:25:35	72	12335.0	43.899								
	17:02:22	0:01:32	3:25:55	92	12355.0	45.53423								
	17:02:46	0:01:56	3:26:19	116	12379.0	44.57772								
	17:25:34	0:24:44	3:49:07	164	13747.0	42.62378								
Run 6														
Particle diameter (mm)	**17:25:51**		3:49:24	0.0	13764.0									
	17:25:57	0:00:06	3:49:30	6	13770.0	3.618862	3.489112	2.104013	3.354346	2.1474				
	17:26:16	0:00:25	3:49:49	25	13789.0	5.44949	5.51677	4.294799	2.783348	3.669478	2.783348			
	17:26:22	0:00:31	3:49:55	31.0	13795.0	6.043319	3.326737	3.515445						

Appendix A: Solid Hydrogen Experiments for Atomic Propellants
Data from image analyses

Bryan Palaszewski
NASA Glenn, MS 5-10
05/30/2001

Solid Hydrogen Experiments for Atomic Propellants

Particle sizes from Solid Hydrogen video observations

Dewar Diameter = 12.4375 in.

Dewar inside diameter = 12 and 7/16 inches

Particle size calibrations
Run 1-3 at 72 dpi. = 508,664 pixels
Run 4-5 at 72 dpi. = 538,483 pixels
Run 6-7 at 72 dpi. = 541,063 pixels

Run 7
Particle diameter (mm)

17:58:51		4:22:24	0.0	15744.0								
17:58:52	0:00:01	4:22:25	1	15745.0	4.524852	5.224849	5.224849	2.750013	3.15602	3.644258	4.251635	
17:58:52	0:00:01	4:22:25	1.1	15745.1	20.57141	15.79073	7.967799	11.15492	11.73439			
17:58:57	0:00:06	4:22:30	6.0	15750.0	4.273272	4.97159	3.912749					
17:59:01	0:00:10	4:22:34	10.0	15754.0	3.354346	2.647492	3.242503	3.0671	4.685073	3.744119	3.719405	3.354346
17:59:03	0:00:12	4:22:36	12.0	15756.0	3.912749	4.877955	4.005922	4.358745	3.381728	4.953004	4.051706	4.504424	4.87795
17:59:06	0:00:15	4:22:39	15.0	15759.0	3.381728	2.71627	3.889106	3.408891	3.669478	3.298898	4.186053		
17:59:07	0:00:16	4:22:40	16.0	15760.0	3.889106	3.213934	3.515445	3.381728	4.163963				
18:06:58	0:08:07	4:30:31	487.0	16231.0	116.8817								
18:11:54	0:13:03	4:35:27	783.0	16527.0	118.8147								
18:14:59	0:16:08	4:38:32	968.0	16712.0	115.586								
18:18:01	0:19:10	4:41:34	1150.0	16894.0	118.6399								
18:21:41	0:22:50	4:45:14	1370.0	17114.0	117.0252								
18:25:17	0:26:26	4:48:50	1586.0	17330.0	118.7262								
18:25:48	0:26:57	4:49:21	1617.0	17361.0	4.743761	4.915623	3.381728	9.679986	4.763163				
18:26:01	0:27:10	4:49:34	1630.0	17374.0	3.381728	2.750013	2.059713	4.763163	4.31622	6.456499			
18:26:11	0:27:20	4:49:44	1640.0	17384.0	2.429505	4.208027	3.768671	12.13993	11.85551				
18:26:17	0:27:26	4:49:50	1646.0	17390.0	22.0378	11.25696	11.73825	11.33046					
18:26:20	0:27:29	4:49:53	1649.0	15773.0	8.717491	7.004606	16.20682	9.080226					
18:26:27	0:27:36	4:50:00	1656.0	17400.0	6.95174	7.043995	3.889106	4.915623					
18:26:54	0:28:03	4:50:27	1683.0	17427.0	8.427005	6.541644	9.221326						
18:31:03	0:32:12	4:54:36	1932.0	17676.0	148.249	28.75913	13.83032						
18:32:13	0:33:22	4:55:46	2002.0	17746.0	151.8933								
18:35:02	0:36:11	4:58:35	2171.0	17915.0	23.41355	14.60863	11.72252						
18:39:04	0:40:13	5:02:37	2413.0	18157.0	32.94422	7.512831	3.036882	4.028879					

Page intentionally left blank

APPENDIX B

SOLID HYDROGEN VIDEO IMAGES: MARCH 23, 1999

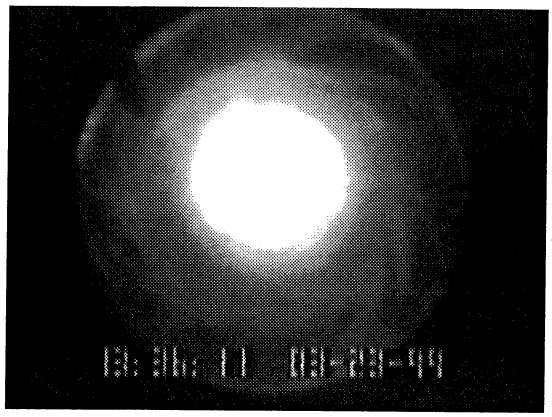

Figure B1.—Solid hydrogen images: Run 1 – 13:36:11.

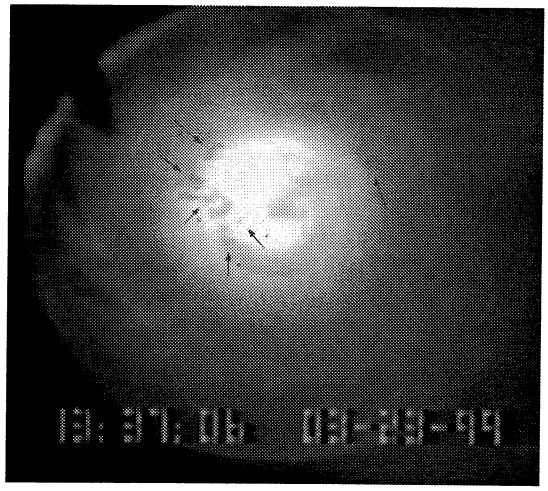

Figure B2.—Solid hydrogen images: Run 1 – 13:37:06.

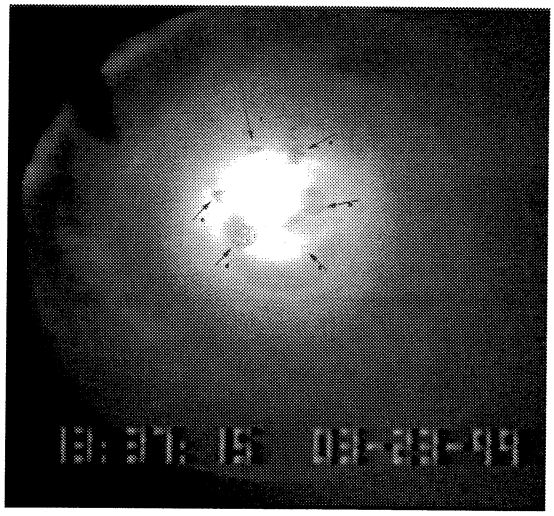

Figure B3.—Solid hydrogen images: Run 1 – 13:37:15.

Figure B4.—Solid hydrogen images: Run 1 - 13:37:28

Figure B5.—Solid hydrogen images: Run 1 - 13:38:54

Figure B6.—Solid hydrogen images: Run 1 – 13:41:44

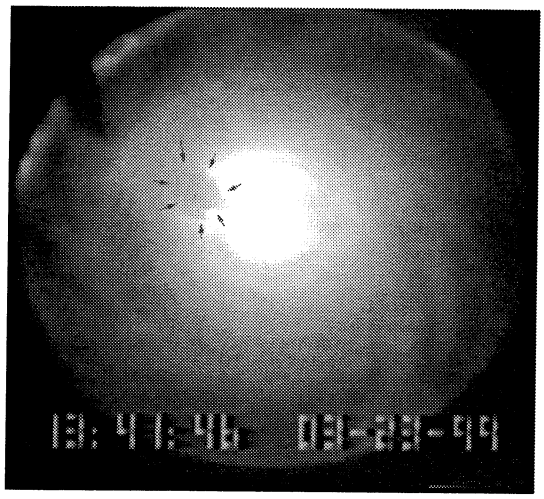

Figure B7.—Solid hydrogen images: Run 1 – 13:41:46.

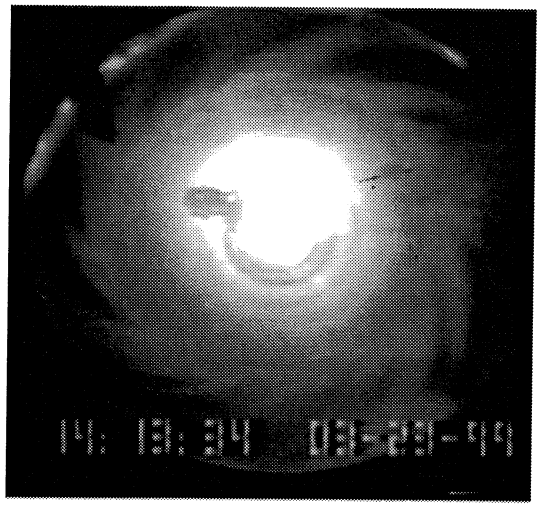

Figure B8.—Solid hydrogen images: Run 2 – 14:13:34.

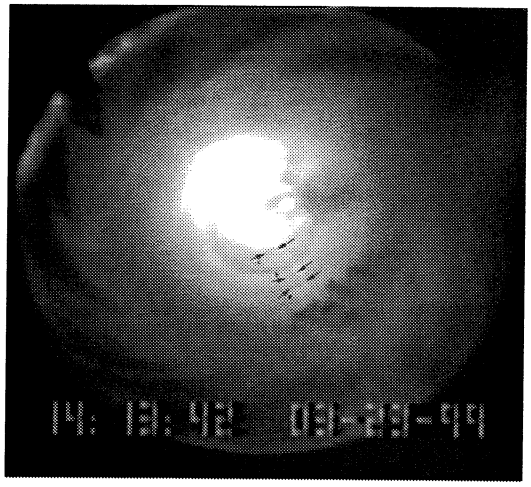

Figure B9.—Solid hydrogen images: Run 2 – 14:13:42.

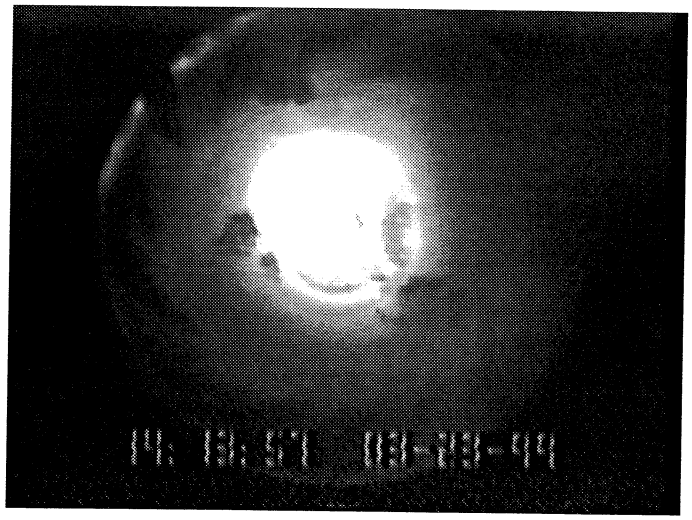

Figure B10.—Solid hydrogen images: Run 2 – 14:13:57.

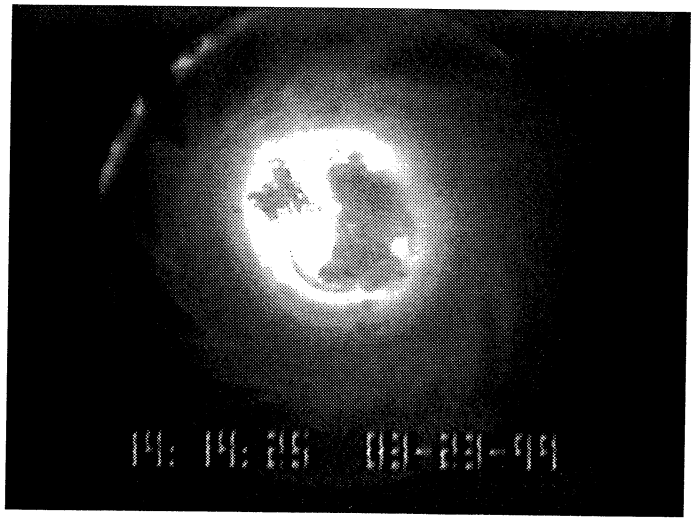

Figure B11.—Solid hydrogen images: Run 2 – 14:14:25.

REPORT DOCUMENTATION PAGE

Form Approved
OMB No. 0704-0188

1. AGENCY USE ONLY (*Leave blank*)	2. REPORT DATE	3. REPORT TYPE AND DATES COVERED
	January 2002	Technical Memorandum

4. TITLE AND SUBTITLE

Solid Hydrogen Experiments for Atomic Propellants: Image Analyses

5. FUNDING NUMBERS

WU–713–74–10–00

6. AUTHOR(S)

Bryan Palaszewski

7. PERFORMING ORGANIZATION NAME(S) AND ADDRESS(ES)

National Aeronautics and Space Administration
John H. Glenn Research Center at Lewis Field
Cleveland, Ohio 44135–3191

8. PERFORMING ORGANIZATION REPORT NUMBER

E–13101

9. SPONSORING/MONITORING AGENCY NAME(S) AND ADDRESS(ES)

National Aeronautics and Space Administration
Washington, DC 20546–0001

10. SPONSORING/MONITORING AGENCY REPORT NUMBER

NASA TM—2002-211297
AIAA–2001–3233

11. SUPPLEMENTARY NOTES

Prepared for the 37th Joint Propulsion Conference and Exhibit cosponsored by the AIAA, ASME, SAE, and ASEE, Salt Lake City, Utah, July 8–11, 2001. Responsible person, Bryan Palaszewski, organization code 5830, 216–977–7493.

12a. DISTRIBUTION/AVAILABILITY STATEMENT

Unclassified - Unlimited
Subject Categories: 15, 20 and 28 Distribution: Nonstandard

Available electronically at http://gltrs.grc.nasa.gov/GLTRS

This publication is available from the NASA Center for AeroSpace Information, 301–621–0390.

12b. DISTRIBUTION CODE

13. ABSTRACT ***(Maximum 200 words)***

This paper presents the results of detailed analyses of the images from experiments that were conducted on the formation of solid hydrogen particles in liquid helium. Solid particles of hydrogen were frozen in liquid helium, and observed with a video camera. The solid hydrogen particle sizes, their agglomerates, and the total mass of hydrogen particles were estimated. Particle sizes of 1.9 to 8 mm (0.075 to 0.315 in.) were measured. The particle agglomerate sizes and areas were measured, and the total mass of solid hydrogen was computed. A total mass of from 0.22 to 7.9 grams of hydrogen was frozen. Compaction and expansion of the agglomerate implied that the particles remain independent particles, and can be separated and controlled. These experiment image analyses are one of the first steps toward visually characterizing these particles, and allow designers to understand what issues must be addressed in atomic propellant feed system designs for future aerospace vehicles.

14. SUBJECT TERMS

High energy density propellants; Atomic propellants; Rocket propulsion; Cryogenics; Rocket propellants

15. NUMBER OF PAGES

30

16. PRICE CODE

17. SECURITY CLASSIFICATION OF REPORT	18. SECURITY CLASSIFICATION OF THIS PAGE	19. SECURITY CLASSIFICATION OF ABSTRACT	20. LIMITATION OF ABSTRACT
Unclassified	Unclassified	Unclassified	